

A Hybrid Rapid Pattern Manufacturing System for Sand Castings

Matthew C. Frank, Frank E. Peters, Xiaoming Luo, Fanqi Meng, Joseph Petzelka

Department of Industrial and Manufacturing Systems Engineering
Iowa State University, Ames, IA, 50011, USA

Abstract

This paper presents a Rapid Pattern Manufacturing system developed for the sand casting process. It involves both additive and subtractive techniques whereby slabs are sequentially bonded and milled using layered toolpaths. As such, patterns are grown in a bottom-up fashion, both eliminating the need for multi-axis operations and allowing small features in deep cavities. Similar approaches exist in the literature; however, this system is specifically targeted at large wood and urethane sand casting patterns. This method introduces a novel support structure approach by integrating a flask into the pattern build process. We also present adaptive slicing algorithms that optimally place layer transitions to avoid thin sections near flats, peaks, and valleys or where interaction with chemically bonded sand could be problematic. The system has been implemented in an automated machine capable of producing patterns in excess of several thousand pounds. Preliminary testing of the system in the development of next generation military equipment is presented in a case study.

Introduction

Sand casting is utilized in the manufacturing of a wide range of metal part sizes, from one to several thousand pounds. Even though sand casting has been used for centuries, it is still one of the most important manufacturing processes today. A key element in the sand casting process is the pattern used to form the mold cavity in sand. Once a pattern is made, tens, hundreds or sometimes thousands of molds can be made; each producing a part. There is a strong motivation to use a rapid prototyping technology for pattern manufacturing, especially for short runs or prototyping where the costs of a pattern cannot be easily justified. However, there are limitations in the current RP technologies mostly related to size constraints and materials available. Most sand casting patterns are made from wood, although some are made of urethanes and metals. Pattern making is considered a highly skilled task and most patterns today are made by specialty pattern shops that serve the foundries, although some foundries still maintain pattern making departments. In early times, patterns were made manually by craftsmen using lathes, mills and other woodworking machines. In some cases, the pattern shop not only creates, but also designs the pattern geometry given the desired part geometry. For example, the original designs of the parts need to be modified to determine parting lines, design cores, apply shrink rules and add draft to surfaces for the subsequent pattern geometry. The emergence of modern CNC machines has reduced the need for hand-made or manually processed patterns; however, this has only shifted the requirements of the pattern makers to high-skilled NC programmers and machine operators. Using a CNC router or milling machine provides the necessary geometric and material capabilities for the pattern industry; yet a truly automated or *Rapid* technology is still not available. Rapid Prototyping & Manufacturing (RP&M) techniques emerged only a few decades ago. Early adopters of some technologies were pattern making shops that needed a better method for testing part and/or pattern designs. This allowed different shrink, draft and gating systems to be tested by making a few sand molds and pouring metal. Once the design was finalized, a durable pattern could be manufactured using conventional means.

Related Work

An early technology was Laminated Object Manufacturing (LOM), which could create sand casting patterns that, at least in appearance and size, were very close to patterns used in the foundry. LOM was used for sand casting patterns, wax injection molds for investment casting, and master models for silicone molding (Mueller and Kochan, 1999). Wang et al. (1999) discussed the LOM process for sand casting patterns and concluded that LOM-based rapid tooling yielded about a 50% time and cost savings compared to aluminum tooling, but that some geometry may not be suitable and that errors in the pattern were common. Selective Laser Sintering (SLS) has been used to directly create the sand molds using coated (*croning*) sand. This technique can be used for very low-volume sand casting molds with complex

geometries which would be difficult to create using traditional sand casting mold techniques (Tang *et al.*, 2003). Similar to SLS, Stereolithography (SLA) has been explored as an important technique in the rapid tooling field. The SLA investment casting build structure called QuickCast™ was introduced in 1993 and has been used to create functional parts in a variety of different metals (Jacobs, 1995; Hague *et al.*, 2001). SLA parts have also been used as patterns to prepare RTV molds and epoxy molds for injection molding (DirectAIM) (Karapatis *et al.*, 1997). Fused Deposition Modeling (FDM) has been directly or indirectly used in investment casting; for investment casting using wax FDM parts or to produce RTV molds from FDM plastic parts to create wax investment casting patterns (Lee *et al.*, 2004). Three Dimensional Printing (3DP) has also been used to create sand casting patterns and molds. The Zcast technique from ZCorp was developed in order to print sand casting molds directly (Kawola, 2008). Thermojet printing such as the Sanders ModelMaker has been effectively used for investment casting through the printing of wax. Its small layer thickness enables very smooth part surfaces, but it also increases the manufacturing time greatly and has relegated the technology to small parts such as jewelry (Naitove, 1996). There has been some research in other technologies that use subtractive methods and hybrid approaches using additive and subtractive means. Schaaf (2000) presented a sand mold RP technique using industrial robots. Yang *et al.* (2002) presented a Robotic Machining RP system using a 6-axis robot on a linear track to perform the cutting operation and a rotary platform to position the workpiece. Hur *et al.* (2002) created a hybrid system using machining and deposition. Shape Deposition Manufacturing (SDM) decomposes the CAD models into sections that can be deposited as near-net shapes and then machines each to net-shape before depositing and shaping additional material (Merz *et al.*, 1994).

Solution Methodology

A proposed methodology for Rapid Pattern Manufacturing (RPM) is presented in this section. The basic premise is to utilize a combined additive and subtractive approach in order to take advantage of accepted materials used in pattern making, while enabling very simplified toolpath and process planning so that it can be automated. The concept is to stack “slabs” of material which are subsequently machined to specified “layer” heights and with the required 3D geometry of only that layer. As such, very deep and complex patterns can be machined using considerably short tools. The process planning is reduced to a set of 2- and 2½-D toolpaths for each layer. For each layer, a face mill reduces the *slab* to a *layer* height and then a sequence of flat- and ball-milling operations using waterline toolpaths generate the 3D surface geometry. The basic steps of the process are illustrated in Figure 1.

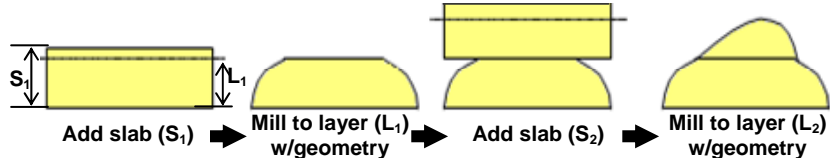


Figure 1 – Basic steps in the Additive/Subtractive approach

Machining each slab to a particular layer thickness serves dual purposes; 1) it creates an accurate flat surface to ensure proper bonding of the subsequent layer and control over the part height and 2) it allows control over where the “seams” occur along the build height. The Additive/Subtractive Rapid Pattern Manufacturing system presented in this paper is designed for 3-axis, single-sided milling. As such, the process is suited mainly for the creation of two-part patterns for the metal casting industry. As partly an academic exercise, we include one undercut geometry (flat surface) for layer placement consideration, since they can be effectively created using an appropriate placement of slabs and layers. However, there are practical instances to justify this, since riser elements (used in pattern design for properly filling a casting) are sometimes implemented as loose components that may have undercut features. In these cases considering undercut flats in the algorithm has practical, albeit not straightforward uses.

The advantage of this rapid pattern manufacturing method may not be obvious, as many in the industry currently use a similar approach with much larger “slabs”, whereby blocks of material are glued together and then machined altogether. The advantage to our proposed method is two-fold 1) we reduce the process planning step from a large machining process plan to simpler, individual layers and 2) most

important, one can feasibly machine an entire pattern with very deep cavities and small features (illustrated in the example of Figure 2. Using this additive/subtractive approach, we can *always* use short, small diameter tools as needed, regardless of depth. Collision conditions typically avoided using 5-axis systems are eliminated altogether in our approach. As shown in Figure 2a, a large slab or solid block approach will lead to inaccessible regions. In contrast, our approach allows a small tool to access small regions, since the subsequent (higher) layers have not yet been added. In the laboratory, we have demonstrated this by making as small as 3mm features (interior radii) close to 1 meter deep in a pattern cavity. A sample pattern for a military component is illustrated in the implementation section; a smaller pattern, with only ~1meter x-y by 0.5meters deep. In theory, the system has very few limits on feature size, since we can control layer depth; hence, the maximum length tool required (short tools can have small diameters as needed, long tools cannot).

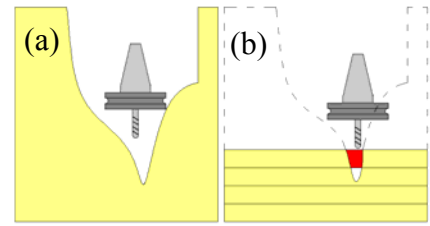


Figure 2 - Deep cavity example (a) large slab or solid block approach causes collision, (b) Layer based approach

The specific problem addressed in this paper is choosing the thickness of the layers comprising each build, based on the slab thickness and the part geometry. As in many additive RP systems, a uniform layer thickness could be used, yet this may result in in-process failures and/or problems in the final quality of the pattern. These machining conditions have resulted in fractured, chipped and/or rough surfaces on wood patterns, or exposed adhesives at layer interfaces. Laboratory experiments have shown that the variable layer placement improves the process significantly; resulting in the successful processing of complex patterns with good surface finishes. This problem of layer placement in RP is not new, however, it is typically not motivated by the same processing requirements. Previous researchers have studied layer thickness in additive/subtractive manufacturing, such as Hur, et al (2002) who presented a hybrid rapid prototyping system using machining and deposition based on a STEP feature model. In a layer based robot machining system presented by Chen and Song (1999), layer thickness is determined based on the feature visibility and slab thickness. Binnard and Cutkosky (1998) utilized a pre-defined basic shape library to facilitate layer thickness planning for SDM. Pinilla, et al (1998) presented another layer thickness method in SDM which was based on the analysis of all silhouette edges that denote transitions from non-undercut surfaces to undercut features. Chang, et al (1999) presented a layer thickness planning approach based on surface splitting. The Free Form Thick Layered Object Manufacturing (FF-TLOM) is a technology that enables the fabrication of large shapes from thick layers of foam with smooth non-faceted surfaces (Broek *et al.*, 2002). The Solvent Welding Freeform Fabrication (SWIFT) process repeats the cycle of solvent welding and CNC contour machining on material sheets (Cormier and Taylor, 2001; Taylor *et al.*, 2001). The uniform stock layer thickness in SWIFT is limited by the feeding system, which introduces geometric error (Yang *et al.*, 2002). Song, et al (2005) presented a direct approach for freeform fabrication of metallic prototypes by 3D welding and milling. Adaptive slicing (Sabourin *et al.*, 1997; Tyberg and Bohn, 1998) also deals with the layer thickness problem; however, the layer thickness definition in the adaptive slicing is different from the layer thickness in this paper. The objective of layer thickness decisions in adaptive slicing is to enable contours in each slice to best represent the part geometry in an efficient manner. However, the layer thickness decision in the proposed Rapid Pattern Manufacturing system is to ensure part geometry is machined effectively, given the geometry of the pattern and the tools and materials used to create the pattern. In previous work, most researchers have considered layer thickness with a motivation of part geometry realization (to make it possible to create the geometry), while some have also considered the material slab thickness constraint. In the proposed Additive/Subtractive Rapid Pattern Manufacturing system, geometry realization is not a problem in theory; two-part patterns for casting components with a definable parting line is not a problem. In contrast, this work is motivated by in-process failures and the final surface quality and strength of the pattern, which we believe can be significantly affected by layer thickness/layout. The problem is to develop an algorithm that will take as input the surface geometry of the desired part (pattern/mold/etc.)

and determine an effective sequential strategy for applying slabs and creating layer thicknesses. The general solution methodology involves several key areas of investigation including; 1) determining a set of factors affecting layer thickness decisions, 2) evaluating the input geometry to determine important “*features*” of the geometry, 3) conducting a *feature* height analysis, and 4) determining layer thicknesses appropriate for each unique combination of *feature* heights. It should be noted that although the term “*feature*” is referred to in this paper, the goal of the research is to provide a more or less “*feature-free*” input requirement. That is, typical *feature-based* approaches assume that a part model is pre-defined by a set of “*features*” such as holes, planes, slots, cavities, bosses, etc. Therefore, when this paper refers to *features*, it is in the sense of geometric characteristics of the part geometry, rather than traditional constructive solid geometry.

Factors affecting layer thickness

The main factors affecting the layer thickness decision in this Rapid Pattern Manufacturing are based on a few assumptions about the general system setup. In this work, the following process and setup is proposed: 1) thick slabs of material are stacked and bonded on a build platform 2) a 3-axis CNC mill/router machines each slab to a flat layer of designated height and forms the part surfaces within that layer, and 3) a set of cutting tools is available, with lengths as long as the slab is thick, or the maximum layer thickness, as required. This paper proposes that the layer thickness criteria are then based on 5 factors; (1) *Minimum cutting tool length*, (2) *Material slab thickness*, (3) *Part geometries*, (4) *Slab and bonding strength*, and (5) *Freeform surface slope*. The minimum cutting tool length from the set of available tools determines the cutting depth for the system; therefore the maximum layer thickness is constrained by this value. The layer thickness must obviously be less than or equal to the material slab thickness. With respect to part geometries, as shown in Figure 3, **Plane I** can be created; however, **Plane II** can only be created if a layer transition occurs precisely at this height. This is only possible when the plane is parallel to the faces of the slab (perpendicular to the stacking direction). Any other down-facing features, such as **Plane III**, cannot be fabricated by this system. When machining, cutting forces can be sufficient to damage a very thin layer, regardless of the bonding strength of the adhesive, or the thin section may vibrate if bonding is not complete. In addition, it is undesirable to have the adhesive exposed as a large surface on the part. In practice, these are potential places where chemically bonded sand could stick to the pattern. These reasons make it necessary to have a minimum criterion for the thickness of each layer.

Feature Analysis: A “*feature*” in this paper is loosely defined as a portion of a part having some machining significance and can be fabricated using 3-axis single-sided machining/routing. According to this definition, there are obviously countless surface shapes that could be considered features. In order to simplify the problem, these features are divided into 3 major groups, Type I, Type II and Type III features. Type I features include local peaks, local valleys and up-facing flats. Type II features are limited to planes having a normal in the $-z$ direction. Finally, a Type III feature is a freeform surface with a shallow slope. As illustrated in Figure 4, a local valley exists as the bottom of a slot (Figure 4c) while local peaks exist on the top of the spherical and rounded entities (Figures 4a,c). The up-facing and down-facing flats are simply flat surfaces with normals in the $+z$ or $-z$ direction, as illustrated in Figures 4b,d. The position of a Type I feature is directly related to the thin layer problem described in the previous section. These heights along the z -axis must be found such that layer transitions at

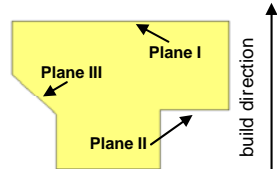


Figure 3 – Basic part geometries

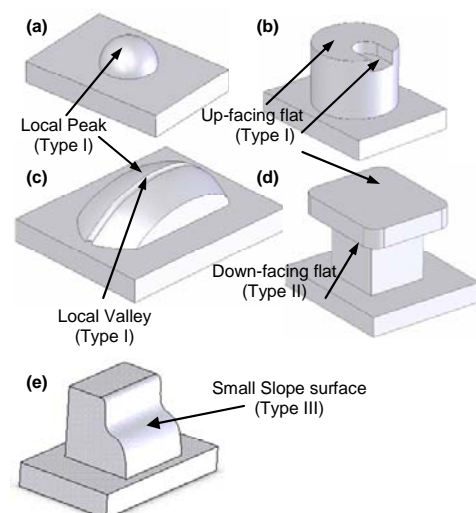


Figure 4 – Feature Examples

these heights are avoided. In contrast, Type II features (Figure 4d) dictate precisely where a layer transition must occur, since it is impossible to create these undercuts by 3-axis machining along the z-axis. Therefore, the bottom side of the slab actually becomes the down-facing flat of the Type II feature. Of course, this also implies that the surface accuracy of the Type II entities is dependant on the slab surfaces, since they will not be machined surfaces. The reader will note that the Type II feature (a down facing plane) is included in this system because it is possible to create them; however, if the system is used for a purpose such as a sand casting pattern Type II features will not exist because they cannot release the sand mold, unless they are a special case of a loose piece riser that will be cut separately. A Type III feature (shallow sloping surface), affects the machining quality similar to an upfacing flat in that we can be confronted with thin material conditions and/or exposed adhesive. The feature heights are the basis of the layer thickness algorithm, therefore the first step is to calculate these heights. The following section presents methods to determine the location of Type I, Type II and Type III feature heights. The location of these feature heights along the z-direction will be used in conjunction with the slab thickness and layer parameters in order to determine the most effective layout of layer transitions. The goal in layer positioning will be to avoid these critical features.

Type I: Local peaks and valleys: The local peak or valley presents a problem of thin materials in convex or concave surfaces. The local valleys have the potential to expose a considerable amount of adhesive. In practice, this has posed a problem if the resins used in the chemically bonded molding sand for casting react with the adhesive. The problem with peaks can be more catastrophic, as we have experienced material failure during cutting. As shown in Figure 5a when an arbitrary layer placement leaves a small contact patch for the next layer, the machining of the slab may shear off the feature. Granted, the adhesive bond does not typically fail, in fact the cyanoacrylate glues used in the process are stronger than the MDF material; hence, the MDF material fails. Examples of these catastrophic failures are presented in the implementation section.

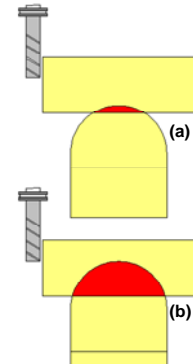


Figure 5 - Local peak issue

For this analysis, we simply analyze the slice geometry from an STL file. Each slice of an STL file contains several loops, or polygonal chains, and each chain defines part of the cross sectional slice of the object at that given layer height. When a loop *appears* or *disappears* from one slice to a successive slice of an STL file, it indicates the emergence or disappearance of what is referred to as a *feature* in this research. The *feature* heights can be obtained by locating these emerging and disappearing loops within the cross sectional slices of the part geometry as the slices are searched along the z-direction. There are several slicing algorithms available (Luo *et al.*, 2001; Choi and Kwok, 2002; Pandey *et al.*, 2003), thus it is easy to obtain the loops from a STL file, and then *feature* heights can be acquired by comparing these 2D loops. In previous work, Tyberg (1998) presents a contour vertical connectivity matching method. The method computes the intersection of two contours which belong to the same sub-slab. However, this approach becomes computationally expensive if many contours exist in each slice. In contrast, we will use a two-step method to speed up the local peak and valley search process. If the numbers of loops in two adjacent slices are different, there must be a feature appearing and/or disappearing. Of course, if the number of loops in these two adjacent slices are the same, it does not necessarily follow that there are no feature changes between them. For example, if an equal number of features appear and disappear simultaneously, then the total loop count for each slice will be the same. Therefore, the first step is to check the numbers of loops in these two adjacent slices. If numbers are different, a disconnection is detected. If the loop numbers are equal a containment evaluation across the slices is performed to assess if a feature is present. This containment relationship analysis is based on a *Point Containment Assumption*, as follows: *If two points having the same coordinate value in the x-y plane are located separately in two planes bounded by line loops on adjacent cross sectional slices, then these two loops are assumed to be from the same part body.* However there is an exception in reverse: As shown in Figure 6, planes S and S' are bounded by line loops from two different part bodies, and there are

two points p and p' with $p \subset S$, $p' \subset S'$. This exception exists only when the distance separating loops is less than the resolution of the slicing algorithm. One simple, but costly method to solve this problem is to use an extremely small slice spacing; however, that could be computationally expensive for tall parts. Of course, the precision of feature detection for our algorithm is decided by the slice resolution; if slice spacing is large, feature height precision suffers. In order to quickly and accurately locate the feature heights, a *Halving Algorithm* (Matthews and Fink, 2004) is adopted. In this manner, a relatively low resolution slice spacing (~ 0.1 inch, 2.54mm) can be used to initially search for features, and then a smaller resolution (~ 0.01 inch, 0.254mm) is used to precisely locate feature heights. In reality, the probability of having the same amount of features disappear and appear at the same z height is very small. Therefore, the probability for this connectivity detection algorithm to get to step 2 is small, making the method more computationally efficient.

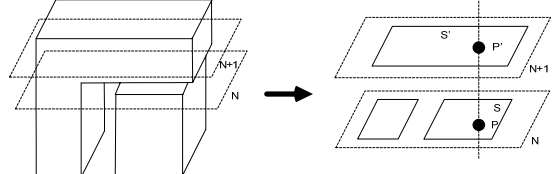


Figure 6 – Exception to point containment assumption

Type I: Up-facing flats: The halving process described above is appropriate for determining heights of local peaks and valleys; however, it is inefficient and inaccurate in finding the exact height of a horizontal plane. In the case of up-facing flat features, it is known that there must be some facet with its normal parallel to the $+z$ axis direction (has a $(0,0,1)$ normal vector, as illustrated in Figure 7a). Therefore, the facet normals of the STL file are searched to locate these potential heights of up-facing flats. In related work, Emmanuel (1996) searched for continuous groups of triangle facets which share the same z height to detect horizontal areas. It should be noted, however, that some small triangular facets created to fill holes in the STL model (post-process repair algorithms), may have the same normals, but do not necessarily represent a flat planar feature (Figure 7b). Another issue is that a small up-facing facet could occur at the tangent “peak” of a freeform or otherwise curved feature. A method to filter these instances is as follows: 1) if two or more adjacent triangles have $+z$ normal, then they exist on an up-facing flat feature (avoids detecting peaks) and 2) if only one triangle whose normal is in $+z$ direction is found, and one dimension of the triangle is significantly small (smaller than the chordal deviation of the STL model), this triangle is not part of up-facing flat feature (avoids triangles added via repair programs). For example, vertex P on the triangle in Figure 7c is very close to the edge L , because this is a very thin triangle added during STL generation/repair. Obviously, this cutoff value can vary depending on the scale of the model and chordal deviation, but it should be a straightforward parameter to establish. Once all local peaks and valleys and up-facing features are determined, their heights are stored into what will be called **Data Set I**. This data set helps determine candidate locations for layers to exist throughout the build height. Although they (peaks, valleys and planes) are located in one data set, they are not treated equally, depending on how close together they exist along the build height. In the case where a local peak or local valley height is within a default distance to an up-facing plane, the local peak or local valley feature height is deleted from **Data Set I**. This approach is employed because an up-facing flat feature is more critical for layer placement as it generally has larger surface area (at the designated z -height), compared to a local peak or valley, hence it is more important to avoid a large area of exposed bonding material as a pattern surface.

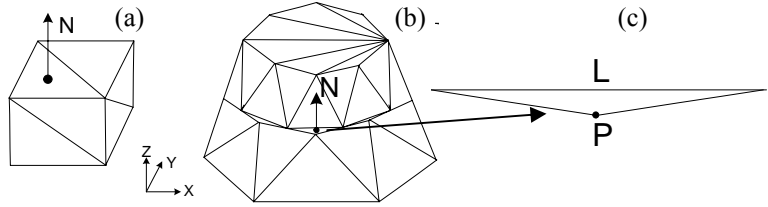


Figure 7 – Detecting up-facing flat; (a) up facing flat, (b) small up-facing facet not on a plane, (c) parameters to define small facets

Type II: Down-facing flats: Both the down- and up-facing flats have normals parallel to the z axis, albeit in opposite direction. Therefore the **Type II** feature height analysis method is the same as the method for up-facing flat height analysis described above; but leads to placing down-facing flat heights into a second set called **Data Set II**. As opposed to the up-facing flat heights in **Data Set I**, for each down-facing flat in

Data Set II, there must be a new layer at that height in order for the down-facing flat to be generated by the bottom face of the material slab.

Type III: Shallow Sloping Freeform Surfaces: The STL file format approximates freeform surfaces with many triangular facets; hence, the idea of analyzing slopes of surfaces is reduced to simply analyzing the triangles of the STL file, and all points in each triangle facet have the same slope. The motivation to study this freeform surface shape is similar to avoiding up facing flat, as a shallow surface approaches the same characteristic. As shown in Figure 8, an arbitrary layout may result in very thin material. Assuming some level of incomplete adhesion (as stated previously, experienced in the laboratory), these thin regions are potentially sheared off during cutting. It should be noted that this problem is similar to the *local peak* condition illustrated above (Figure 5), where a thin section fractures under cutting forces. The angle of the facets to the horizontal is found and we establish a minimum value experimentally/experientially based on the strength of the pattern material. In laboratory experiments a nominal value of 15° has successfully avoided chipping in Medium Density Fiberboard (MDF), a material that is suitable for sand casting patterns. Higher strength materials such as hardwoods, RenBoard, or of course metals would allow smaller shallow facet angles.

One subtle difference between **Type III** features and the other two features discussed above is that a **Type III** feature often covers a range along the Z direction since the freeform surfaces are approximated by many small triangles in the STL file format, rather than a distinct height of a peak, valley or flat. The total range of **Type III** features along the Z direction are determined by the range of z-heights for the vertices of all shallow slope facets and these feature ranges are stored in **Data Set III**. It should be noted that material slab heights are limited therefore; a **Type III** feature may not always be avoided in layer height calculations. In this case, the methods of the secondary approach presented later in this paper are utilized.

Layer thickness algorithm

The proposed layer thickness algorithm defines locations where slabs of material are bonded in the additive portion of the process. After a slab is placed and bonded onto the stack, the subtractive process not only creates the 3D geometry of the layer, but also mills the slab to the designated *layer* thickness. Although the slabs are typically of uniform thickness, layer thicknesses will vary throughout the part as required. Slab thickness could in fact also be varied, if for no other reason than to reduce waste (reduce the amount of material removed when the layer height is much smaller than the slab thickness). For each layer, the slab could simply be chosen as the smallest slab that is thicker than the current layer thickness. This small improvement is ignored in this paper, as it does not change the layer thickness algorithm development. Moreover, allowing a variety of slab thicknesses adds considerable complexity to the Rapid Pattern Manufacturing System; one would need to be able to store, pickup and place a variety of thicknesses. In the current system, we have only used a uniform slab thickness based on available pattern materials in sheet form (i.e. $\sim 0.75''$ MDF boards).

Primary layer thickness strategy for Type I features: Firstly, we establish a minimum thickness allowable for any layer, denoted MT_{min} . This is a default value dependent on the material strength and bonding strength. The maximum layer thickness LT_{max} is set to the minimum value between the slab thickness ST and tool length TL ; $LT_{max} = \text{Min}(ST, TL)$, where MT_{min} is the minimum material thickness, ST is the material slab thickness and TL is the minimum tool length. The primary layer thickness strategy for each Type I feature is: There should be no deposition within a z region ($H1_m - MT_{min}, H1_m$) which is

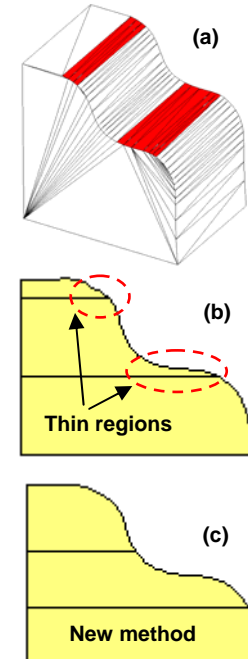


Figure 8 - Shallow slope surfaces

called a *Non-Deposition* region, where: Hl_m is the m^{th} Type I feature z height. To begin, *Non-Deposition* regions are calculated and stored in data set ND_j , which is the Non-Deposition z height region (ND_{j-}, ND_{j+}). Each ND_j includes two values: the upper limit ND_{j+} , and the lower limit ND_{j-} ; where $ND_{j-} = Hl_m - MT_{min}$ and $ND_{j+} = Hl_m (j = m)$. If two

Non-Deposition regions overlap, they are combined as $ND_j = ND_{(j-1)} (If ND_{j-} < ND_{(j-1)}^+)$. If there exist Type II entities in the range of a *Non-Deposition* region, the *Non-Deposition* region is then divided into two *Non-Deposition* regions at these Type II entity z heights, since a Type II feature has higher priority. This division operation avoids layer placement conflicts between Type II entities and *Non-Deposition* regions. The sample part illustrated in Figure 9 has seven Type I *feature* entities; hence there are seven *Non-Deposition* regions. It happens that some *Non-Deposition* regions in this example connect; hence only two *Non-Deposition* regions are formed after combining. *Secondary layer thickness strategy for Type I features*: After all combinations, some *Non-Deposition* regions may exceed the height of the material slab thickness. This indicates that it is not possible to have a layer covering the entire *Non-Deposition* region. When this problem occurs, the primary layer thickness strategy for Type I *feature* fails, and a secondary layer thickness strategy is employed. When the height of a Type I *feature* is above the layer position by MT_{min} , bonding strength and material strength are assumed sufficient to ensure proper machining and part quality. However if the distance between the feature and the layer position is less than MT_{min} , the quality/value of a layer height choice is decided by two factors: 1) the distance between the feature and the layer position (DT), and 2) the cross section loop area (A) at the particular layer z height. When two Type I *feature* entities connect to each other, the best position to place a layer along this *Non-Deposition* region is exactly at the lower entity position, which has the largest DT and A for the upper entity. Therefore, the lower *feature* positions are evaluated using a simple cost objective function to quantify the benefits of placing layers at these positions; $Q = \alpha * DT + \beta * A$, where: α is a material coefficient (unit: $(inch)^{-1}$), β is a bonding/adhesive coefficient (unit: $(inch^2)^{-1}$), DT is the distance between *feature* and layer position, and A is the cross section loop area at the layer height. The material coefficient α and bonding/adhesive coefficient β are weight parameters which specify the influence of DT and A on the Q -value. Currently, these two coefficient values were acquired through experimental efforts with medium density fiberboard (MDF) as the pattern material and Cyanoacrylate as the adhesive. For general implementation, there is no theoretical optimal weight values that would have a straightforward derivation. Rather, they would need to be tuned experimentally based on the pattern material and adhesives of choice (stronger or weaker materials or glues could dictate arbitrarily different weights). This heuristic approach does not necessarily yield an optimal solution based on Q -value, especially since it may result in an excessive number of layers in a *Non-Deposition* region, driving up material and adhesive costs.

Then, a branch-and-bound algorithm was adopted to minimize the number of layers, while maximizing the Q -value of possible positions in the *Non-Deposition* regions. The first level selects the number of layers placed in the *Non-Deposition* region. The search starts from the theoretical minimum number of layers, which is $L_{min} = UR [(ND_{j+} - ND_{j-}) / LT_{max}]$, where $UR(x)$ is an operation that calculates the smallest integer $\geq x$. Next, feature heights are searched in sequence of increasing Q -values for possible layer placement solution. Consider the ND_2 in Figure 9 for example. The height of ND_2 is 1.0 inch, LT_{max} is 0.8 inch, f_6 (which has the largest Q -value) is 0.1 inch from the bottom of ND_2 , and f_5 has the second largest Q -value, which is 0.25 inch from the bottom of ND_2 . For level 1, the minimum layer number needed to cover the ND_2 in theory is $UR(1.0/0.8) = 2$. Then, the level 2 starts from f_6 . If $f_6 = 1$, at least one more layer is required since $UR((1.0-0.1)/0.8) = 2$, and the total number of layers is greater than 3.

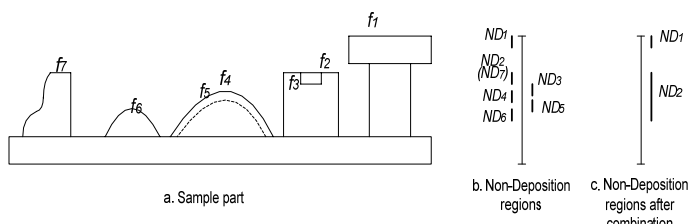


Figure 9 – *Non-Deposition* region combination

Therefore, $f6 = 0$. In level 3, if $f5 = 1$, no more layers are required, since $UR((1.0-0.25)/0.8)=1$, and the total number of layers required is 2 which is equal to the minimum theoretical number of layers. At this point, the search process is completed and layer positions in the *Non-Deposition* region are stored into **Data Set II**, which stores the **Type II feature** heights. Layer placement in the *Non-Deposition* region is actually similar to the **Type II feature** problem, in which there must be layers placed at these positions to cover *Non-Deposition* regions.

Overall Layer Thickness Algorithm: The overall layer thickness algorithm places layers in a bottom-up fashion. To begin, the bottom of the CAD model of the pattern is positioned at $z = 0$, and the initial start position is set to $H_c = 0$, where H_c is the current tentative layer z height. The current layer number i is set to 1, H_{10} is set to 0. When the search begins, the current tentative layer height is set to one maximum layer thickness (LT_{max}) higher than the previous layer: $H_c = H_{i-1} + LT_{max}$. Next we determine Layer Thicknesses for Data Set II. Type II features and layer positions in Non-Deposition regions are evaluated first since layers must correspond exactly at these heights in order to create the down-facing flat geometry, or to provide suitable machining quality in the Non-Deposition regions. First, all height data in Data Set II are searched to determine those that are within the height range H_{i-1} to H_c . If multiple heights are possible, the height that is closest to H_{i-1} is the next layer position (H_i), where H_i is the z height of the i^{th} layer. If no such feature height is found, the search continues for Type I feature heights. For Layer thickness for Type I features, if there is a j that meets the condition: $ND_{j-} < H_c < ND_j^+$, then H_c is in the range of a Non-Deposition region. As such, H_c should be moved out of the Non-Deposition region $H_c = ND_{j-}$; else, a layer can be placed at H_c directly. The Non-Deposition regions here are only those less than LT_{max} . If they are greater than LT_{max} , layers are placed directly in the first step. Therefore, Non-Deposition regions above LT_{max} cannot be selected in the second step. Finally, we determine Layer thicknesses for Type III features. For this step, Layers are also placed based on Type III features; however, it occurs that Type I and Type III features may cause conflicts; one cannot always satisfy both Type I and III features simultaneously. Again from experimental tests, Type III features create poor machining conditions, but Type I features more often cause catastrophic failures: hence, Type I features are given higher priority to be satisfied. We will define H_{3o} as the o^{th} Type III feature z height region (H_{3o-}, H_{3o+}). For the H_c from step (b), if there exists an o for $H_{3o-} < H_c < H_{3o+}$ (that is, this H_c is located within the range of a Type III feature), then, the height H_{3o} is tested. If no j exists for: $ND_{j-} < H_{3o-} < ND_j^+$, then H_c is moved to H_{3o-} , or, H_c is kept the same. In this iterative manner, the Type I, Type II and Type III feature searching processes determine the layer thicknesses for the entire part.

Implementation

The layer thickness algorithm has been implemented and several patterns have been created in the laboratory, with chemically bonded sand molds pulled from the patterns and casting performed. The evaluation of the approach presented in this section involves 1) comparing the calculated *feature* heights from the algorithm with design *feature* heights, 2) fabricating sample test patterns to evaluate the efficacy of this layer based approach, and 3) practical testing of the methods in the creation of actual sand casting patterns for a relatively large casting.

Test Sample: The layer thickness algorithm was implemented in C++ on a Pentium 3.0GHz PC running Windows XP. The input to the layer thickness software was an STL file (ASCII, 0.001 inch chordal deviation). A sample part was designed to verify the layer thickness algorithm such that all steps and conditions would be tested. In this example, the material slab thickness (Medium Density Fiber board) was 0.70 inch. Tool lengths are larger than the slab thickness, so LT_{max} is set to 0.70 inch. The minimum layer thickness MT_{min} was set

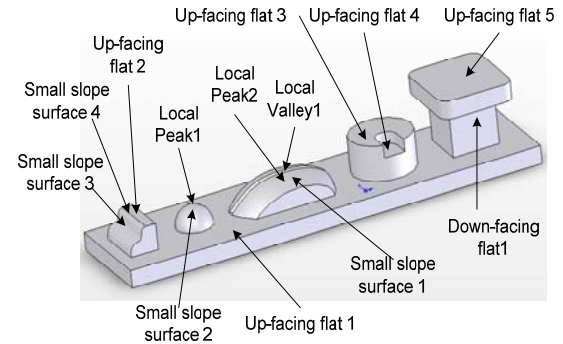


Figure 10 – Sample part 3D model

to 0.20 inch. The material coefficient was 0.7 (Length unit: inch), the bonding coefficient was set to 0.3 (Area unit: inch²) and the small slope surface threshold angle was set to 15°. Figure 10 shows a 3D model of the sample part. Twelve machining features are detected by the layer thickness software, with the positions of these twelve features listed in Table 1.

The small differences between the design positions and detected positions come from two sources. One error source is the approximation inherent with an STL model while the other is from the Halving Algorithm which can only acquire approximate local peak or valley positions. That being said, in this example the differences are less than 0.005 inch and consequently have little influence on the layer thickness evaluation. Layer thickness results are presented in Figure 11. The first layer thickness follows the *primary* layer thickness strategy for a **Type I** feature; and is 0.2inch lower than local *peak 1*. The second layer thickness utilizes the *secondary* layer thickness approach for a **Type I feature**, and the layer thickness calculated from *local valley 1* meets the optimization condition (4) presented in section 2.4.2. The third layer thickness is obtained directly from the **Type II feature's** down-facing *flat 1*. The last layer ends at the top of the part (an up-facing plane). In this example, computation time for this model was ~3 seconds.

Table 1 – Design vs. Detected feature heights (Unit: inch)

Feature	Detected Height	Design Height	Feature	Detected Height	Design Height
Up-facing flat 1	0.3	0.3	Local peak 1	0.653	0.65
Up-facing flat 2	0.7	0.7	Local peak 2	0.803	0.805
Up-facing flat 3	1	1	Local valley 1	0.756	0.755
Up-facing flat 4	1.18	1.18	Small slope surface 1 & 4	0.638 - 0.650	0.624 - 0.650
Up-facing flat 5	1.5	1.5	Small slope surface 2	0.520 - 0.533	0.516 - 0.523
Down-face flat 1	1.2	1.2	Small slope surface 3	0.660 - 0.744	0.652 - 0.744

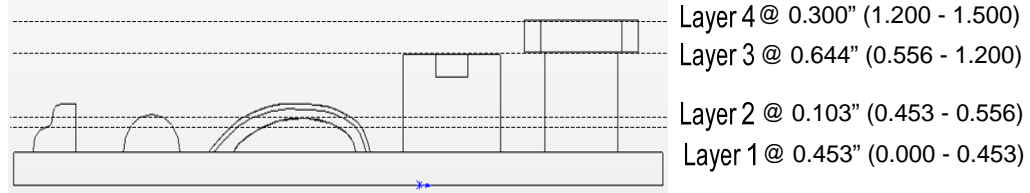


Figure 11 – Sample part layer distribution

Sand Casting Pattern Testing: A Rapid Pattern Manufacturing system has been developed and tested in the Rapid Manufacturing and Prototyping Laboratory at Iowa State University (Figure 12). The system is comprised of 4 major functional elements including; 1) two elevator platforms serving as feed and build chambers with 1.2m³ (1440kg) capacities, 2) a material handling system to clamp, position and compress up to 1.2m² sheets of material, 3) a glue application system, and 4) one off-the-shelf component; a 3-Axis CNC router. A total of 7 controllable axes are utilized in the completely automated processing of patterns. The gluing system utilizes a peristaltic pump which directs cyanoacrylate adhesive through a manifold applicator head. The servo driven build table with 4 ball screws can position the pattern for cutting operations and apply up to 17,000N of force during the 30second gluing compression cycle. The layer thickness algorithm has been implemented in software as a C-hook in the MasterCAM CAD/CAM environment. NC code for each layer and the requisite slab sequencing and facing to layer height data is output from MasterCAM and then processed using customized control system software to drive the machine elements.

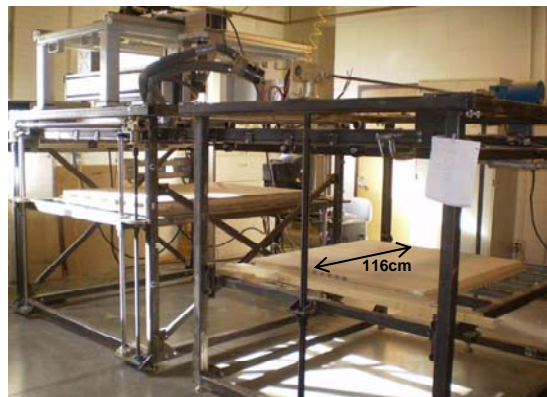


Figure 12 - Rapid Pattern Machine in Rapid Manufacturing and Prototyping Lab at ISU

The system has been utilized to create numerous prototype patterns and most recently for a pattern of a steel cast component measuring over 800x800x300mm. This large sand casting pattern made by the Rapid Pattern Manufacturing machine and the sand mold created from this pattern are shown in Figure 13. Figure 13a, shows the pattern in the latter stages of being machined in the system, illustrating the advantage of using a layer based approach, as it can be seen how the current layer in the picture is breaking through to reveal the deep pattern cavity below. One will note that this pattern is considerably large and deep; however, only a 1 inch (25mm) long end mill was required, since each layer is machined after being stacked. As such, we were able to use as small as a $\frac{1}{4}$ "(6mm) diameter ball mill to access small corner radii, even in the deepest regions of the pattern. Total machining time for this size pattern is currently at approximately 50 hours, or roughly 2 hours per inch (25mm) of z-height on this 116x116cm (slab dimension) pattern build. The process is currently limited by the maximum feedrate of this CNC router (a maximum of ~350ipm (9m/min)) although the pattern material could be machined faster. Figure 13b presents a closer image of interior of the finished pattern; while Figure 13c shows the resulting sand mold pulled from this pattern cavity. This pattern was used to successfully cast a large steel prototype component.

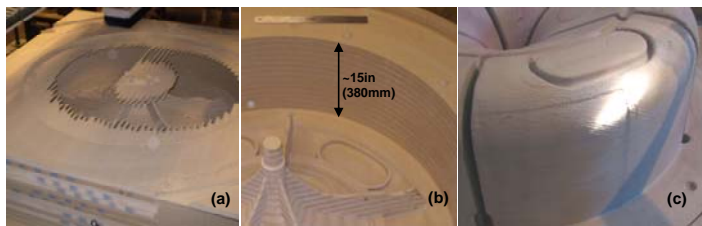


Figure 13 – Example Pattern and Mold; a) Pattern in process machining through a layer and exposing pattern cavity below, b) finished pattern with complex geometry deep in cavity, and c) chemically bonded sand mold pulled from pattern

Conclusion

This paper presented a critical enabling technique in the rapid manufacturing of patterns using an additive/subtractive approach. The research addresses a need for effective layout of layers in this process, as it has been found that layer placement has a significant effect on surface quality of the patterns and more important can avoid catastrophic failure during the machining processes. The algorithm presented deals effectively with the set of feature conditions that must be addressed. Feature creation is not an inherent problem in this system; since the geometry of sand casting patterns has relatively well-known characteristics. The problem arises in the additive/subtractive nature of the process, as this creates temporary geometric problems such as thin webs of material, potential fracture conditions, etc. However, it is also the layer based nature of the process that enables the rapid prototyping of these patterns, since the process planning is greatly simplified; being able to machine each layer with small tools capable of creating small features and no collision conditions.

Acknowledgements

Research was sponsored by the U.S. Army Benet Laboratories and was accomplished under Cooperative Agreement Number W15QKN-06-R-0501. The views and conclusions contained in this document are those of the authors and should not be interpreted as representing the official policies, either expressed or implied, of U.S. Army Benet Laboratories or the U.S. Government. The U.S. Government is authorized to reproduce and distribute reprints for Government purposes notwithstanding any copyright notation heron.

Reference

- Binnard, M. and Cutkosky, M. (1998), "Building block design for layered shape manufacturing", *Proceedings-1998 ASME Design Engineering Technical Conference*, pp. 1-9.
- Broek, J.J., Horváth, I., Smit, B., Lennings, A.F., Rusák, Z., Vergeest, J.S.M. (2002), "Free-form thick layer object manufacturing technology for large-sized physical models", *Autom. in Construction*, Vol. 11 No. 3, pp. 335-347.
- Chang, Y.C., Pinilla, J.M., Kao, J.H., Dong, J., Ramaswami, K., Prinz, F.B. (1999), "Automated layer decomposition for additive/subtractive solid freeform fabrication", *Proceedings of the Solid Freeform Fabrication Symposium*, pp. 111-120.
- Chen, Y.H., Song, Y. (2001), "The development of a layer based machining system", *Computer-Aided Design*, Vol. 33 No. 4, pp. 331-342.

- Choi, S.H. and Kwok, K.T. (2002), "Hierarchical slice contours for layered-manufacturing", *Computers in Industry*, Vol. 48 No. 3, pp. 219-239.
- Cormier, D. and Taylor, J.B. (2001), "A process for solvent welded rapid prototype tooling", *Robotics and Computer Integrated Manufacturing*, Vol. 17 No. 1-2, pp. 151-157.
- Hague, R., D'Costa, G., Dickens, P.M. (2001), "Structural design and resin drainage characteristics of QuickCast 2.0", *Rapid Prototyping Journal*, Vol. 7 No. 2, pp. 66-72.
- Hur, J.H., Lee, K., Zhu-hu, Kim, J. (2002), "Hybrid rapid prototyping system using machining and deposition", *Computer-Aided Design*, Vol. 34 No. 10, pp. 741-754.
- Jacobs, P.F. (1995), "QuickCast 1.1 and rapid tooling", *Proceedings of 4th European Conference on Rapid Prototyping & Manufacturing*, pp. 1-27.
- Karapatis, N.P., Van, Griethuysen, J.P.S., Glardon, R. (1997), "Injection molds behavior and lifetime characterization" *Proceedings of the Solid Freeform Fabrication Symposium*, pp. 317-324.
- Kawola, J. (2008), "Zcast direct metal casting from data to cast aluminum in 12 hours", Website: <http://www.3dprint.no>.
- Lee, C.W., Chua, C.K., Cheah, C.M., Tan, L.H., Feng, C. (2004), "Rapid investment casting: direct and indirect approaches via fused deposition modeling", *International Journal of Advanced Manufacturing Technology*, Vol. 23 No. 1-2, pp. 93-101.
- Leong, K.F., Chua, C.K., Ng, Y.M. (1996), "Study of stereolithography file errors and repair: part 1- generic solution", *International Journal of Advanced Manufacturing Technology*, Vol. 12 No. 6 pp. 407- 414.
- Leong, K.F., Chua, C.K., Ng, Y.M. (1996), "Study of stereolithography file errors and repair: part 2-special cases", *International Journal of Advanced Manufacturing Technology*, Vol. 12 No. 6, pp. 415- 422.
- Luo, R.C., Chang, Y.C., Tzou, J.H. (2001), "The development of a new adaptive slicing algorithm for layered manufacturing systems", *Proceedings of the 2001 IEEE International Conference on Robotics & Automation*, pp. 1334-1339.
- Matthews, J.H. and Fink, K.D. (2004), "Numerical methods: using Matlab", Prentice hall.
- Merz, R., Prinz, F.B., Ramaswami, K., Terk, M., Weiss, L.E. (1994), "Shape deposition manufacturing", *Proceedings of the Solid Freeform Fabrication Symposium*, pp. 1-8.
- Mueller, B. and Kochan, D. (1999), "Laminated object manufacturing for rapid tooling and patternmaking in foundry industry", *Computers in Industry*, Vol. 39 No. 1, pp. 47-53.
- Naitove, N.H. (1996), "Faster, bigger desktop modeler", *Plastics Technology*, Vol. 42 No. 12, pp. 27.
- Pandey, P.M., Reddy, N.V., Dhande, S.G. (2003), "Slicing procedures in layered manufacturing: a review", *Rapid Prototyping Journal*, Vol. 9 No. 5, pp. 274-288.
- Pinilla, J.M., Kao, J., Prinz, F.B. (1998), "Process planning and automation for additive/subtractive solid freeform fabrication", *Proceedings of the Solid Freeform Fabrication Symposium*, pp. 245-258.
- Sabourin, E., Houser, S.A., Bohn, J.H. (1997), "Accurate exterior, fast interior layered manufacturing", *Rapid Prototyping Journal*, Vol. 3 No. 2, pp. 44-52.
- Schaaf, W. (2000), "Robototyping - new rapid prototyping processes for sand casting moulds using industrial robots", *Assembly Automation*, Vol. 20 No. 4, pp. 321-329.
- Song, Y. and Chen, Y.H. (1999), "Feature based robot machining for rapid prototyping", *Proceedings of the Institution of Mechanical Engineers, Part B: Journal of Engineering Manufacture*, Vol. 213 No. 5, pp. 451-459.
- Song, Y.A., Park, S., Choi, D., Jee, H. (2005), "3D welding and milling: part I – a direct approach for freeform fabrication of metallic prototypes", *International Journal of Machine Tools and Manufacture*, Vol. 45 No. 9, pp. 1057-1062.
- Song, Y.A., Park, S., Chae, S.W. (2005), "3D welding and milling: part II – optimization of the 3D welding process using an experimental design approach", *International Journal of Machine Tools and Manufacture*, Vol. 45 No. 9, pp. 1063-1069.
- Tang, Y., Fuh, J.Y.H., Loh, H.T., Wong, Y.S., Lu, L. (2003), "Direct laser sintering of a silica sand", *Materials & Design*, Vol. 24 No. 8, pp. 623-629.
- Taylor, J.B., Cormier, D., Joshi, S., Venkataraman, V. (2001), "Contoured edge slice generation in rapid prototyping via 5-axis machining", *Robotics and Computer Integrated Manufacturing*, Vol. 17 No. 1-2, pp. 13-18.
- Tyberg, J., Bohn, J.H. (1998), "Local adaptive slicing", *Rapid Prototyping Journal*, Vol. 4 No. 3, pp. 118 – 127.
- Wang, W., Conley, J.G., Stoll, H.W. (1999), "Rapid tooling for sand casting using laminated object manufacturing process", *Rapid Prototyping Journal*, Vol. 5 No. 3, pp. 134-140.
- Yang, Z.Y., Chen, Y.H., Sze, W.S. (2002), "Layer-based machining: Recent development and support structure design", *Proceedings of the Institution of Mechanical Engineers, Part B: Journal of Engineering Manufacture*, Vol. 216 No. 7, pp. 979-991.